The Journal of Neuroscience, December 1995, 15(12): 7989–7999

Multiple *Shaker* Potassium Channels in a Primitive Metazoan

Timothy Jegla,[1] Nikita Grigoriev,[2] Warren J. Gallin,[2] Lawrence Salkoff,[1] and Andrew N. Spencer[2]

[1]Department of Anatomy and Neurobiology, Washington University School of Medicine, St. Louis, Missouri 63110 and [2]Department of Biological Sciences, University of Alberta, Edmonton, Alberta, Canada T6G 2E9 and Bamfield Marine Station, Bamfield, British Columbia Canada V0R 1B0

Voltage-gated potassium channels are critical elements in providing functional diversity in nervous systems. The diversity of voltage-gated K^+ channels in modern triploblastic metazoans (such as mollusks, arthropods and vertebrates) is provided primarily by four gene subfamilies (*Shaker, Shal, Shab,* and *Shaw*), but there has been no data from the ancient diploblastic metazoans until now. Diploblasts, represented by jellyfish and other coelenterates, arose during the first major metazoan radiation and are the most structurally primitive animals to have true nervous systems. By comparing the K^+ channels of diploblasts and triploblasts, we may determine the fundamental set of K^+ channels present in the first nervous systems. We now report the isolation of two *Shaker* subfamily cDNA clones, *jShak1* and *jShak2,* from the hydrozoan jellyfish *Polyorchis penicillatus* (Phylum Cnidaria). *JShak1* and *jShak2* express transient outward currents in *Xenopus* oocytes most similar to *Shaker* currents from *Drosophila* in their rates of inactivation and recovery from inactivation. The finding of multiple *Shaker* subfamily genes is significant in that multiple *Shaker* genes also exist in mammals. In *Drosophila,* multiple *Shaker* channels are also produced, but by a mechanism of alternative splicing. Thus, the *Shaker* K^+ channel subfamily had an established functional identity prior to the first major radiation of metazoans, and multiple forms of *Shaker* channels have been independently selected for in a wide range of metazoans.

[Key words:* Shaker, *potassium channel, voltage-gated, jellyfish, Cnidarian, diploblast, triploblast, polyorchis, inactivation]

Electrical excitability is a fundamental property of the neuromuscular systems of metazoans. This property is conferred by a diverse set of voltage-gated (Vg) ion channel proteins that has evolved in concert with neurons and other excitable cells. Neurobiologists have come to appreciate that the surprisingly varied responses of neurons to electrical excitation can in a large part be accounted for by a diverse, but highly conserved, set of Vg potassium channel proteins that are present in most metazoans (Rudy, 1988; Salkoff et al., 1992).

The molecular basis of K^+ channel diversity is well understood in many triploblastic metazoans, including vertebrates (Jan and Jan, 1990; Rudy et al., 1991; Salkoff et al., 1992; Chandy and Gutman, in press), arthropods (Jan and Jan, 1990; Salkoff et al., 1992; Pongs, 1993), and mollusks (Pfaffinger et al., 1991; Quattrocki et al., 1994; Zhao et al., 1994), and has been examined in other triploblasts groups such as annelids (Johansen et al., 1990), nematodes (Wei et al., 1991), and flatworms (Kim et al., 1995). In these organisms, much of the K^+ channel diversity appears to be encoded by four closely related gene subfamilies of Vg K^+ channels: *Shaker, Shal, Shab,* and *Shaw.* However, it has not been clear whether this set of Vg K^+ channels diversified within the triploblastic lineage or whether it was, at least in part, present during the establishment of the nervous system in more primitive metazoans.

The most ancient extant metazoans to have true nervous systems are the diploblasts, organisms such as jellyfish, sea anemones, and comb-jellies. These organisms have only two germinal layers, lacking a true mesoderm. Both the fossil record and molecular phylogenies based on ribosomal RNA sequences place the emergence and diversification of the extant diploblastic phyla well before the appearance of modern triploblasts, during an initial major radiation of metazoan species (Christen et al., 1991; Morris, 1993; Wainwright et al., 1993). Thus, the first nervous systems most likely appeared in one of the latest common ancestors of diploblasts and triploblasts.

Physiological evidence shows that the diploblasts, like triploblasts, have a diverse set of Vg K^+ currents (Anderson and McKay, 1987; Dunlap et al., 1987; Holman and Anderson, 1991; Meech and Mackie, 1993; Przysiezniak and Spencer, 1994), hinting at an early diversification of Vg K^+ channel genes. By examining the molecular diversity of Vg K^+ channels in diploblasts such as jellyfish, we can gain an understanding of the molecular diversity of Vg K^+ channels in the first nervous systems and how it has been conserved or specialized to meet the needs of modern triploblasts with their complex nervous and effector systems.

Using a PCR screening protocol, based on degenerate primers corresponding to the regions most highly conserved between the *Shaker, Shal, Shab,* and *Shaw* subfamilies, we have isolated two *Shaker* subfamily homologs, *jShak1* and *jShak2,* from the hydromedusan jellyfish *Polyorchis penicillatus.* We report the sequences of these K^+ channel subunits and demonstrate remarkable similarity to their triploblastic homologs. These results show that the *Shaker* Vg K^+ channel gene subfamily has been

Received June 14, 1995; revised Aug. 3, 1995; accepted Aug. 7, 1995.

We thank Dr. Aguan Wei for his role in developing our PCR screen, as well as his helpful comments and enthusiasm. The *Shaker H37* clone was kindly provided by Dr. Mark Tanouye, *Shaker B* by Dr. Tom Schwarz, and *Kv1.2* by Dr. David McKinnon. We thank the Bamfield Marine Station for their assistance in collecting and holding jellyfish and maintenance of a *Xenopus* colony. Research was supported by grants from the NIH and MDA to Lawrence Salkoff and from the NSERC to W.J.G. and A.N.S.

Correspondence should be addressed to Timothy J. Jegla, Washington University School of Medicine, Department of Anatomy and Neurobiology, Box 8108, 660 South Euclid Avenue, St. Louis, MO 63110.

functionally differentiated from other Vg K^+ channel lineages at least since the appearance of the nervous system. Thus, the diversity of Vg K^+ channels observed in triploblasts is likely to have arisen during or even prior to the earliest major radiation of metazoan species.

Materials and Methods

Cloning of jShak1 *and* jShak2. Amplification and isolation of fragments of *jShak1* and *jShak2* from *Polyorchis penicillatus* genomic DNA was performed as described in Jegla and Salkoff, 1995. Briefly, the degenerate primers used to generate the fragments were 5′-TCGGAATTCTATGACTACTGTTGG(A\C\G\T)TA(T\C)GG(A\C\G\T)GA-3′ (sense) and 5′-ACTTCTAGAGGTAGTGCTATT(G\A)(T\C)(A\C\G\T)-AG(A\C\G\T)AC(A\C\G\T)CC-3′ (antisense) which are derived from the consensus amino acid sequences of the pore region [MTTVGYG(D/E)] and sixth transmembrane domain [GVL(T/V)TIAL] of Vg K^+ channels. The *jShak1* and *jShak2* fragments obtained in the amplification screen were used to probe oligonucleotide dT primed *Polyorchis* cDNA libraries under high stringency conditions (Butler et al., 1989). Purification of mRNA from neuronally enriched *P. penicillatus* tissue samples and construction of the cDNA libraries in the lambdaZAP II vector (Stratagene, La Jolla) have been described previously (Gallin, 1991). Bluescript SK^- subclones of each positive clone were obtained using Stratagene's *in vivo* excision protocol and sequenced in both directions. This procedure yielded a complete cDNA clone of *jShak1*. However, all *jShak2* cDNAs were truncated, containing only a region encoding S1 through the 3′ end of the coding sequence. The missing 5′ region was obtained by high stringency amplification (95°C 1 min, 60°C 3 min, 30 cycles) of a cDNA bank with 0.5 pmol/μl of an oligonucleotide matching the T7 region of Bluescript 5′-(GCGCGTAATACGACTCACTATAGGG)-3′ and 25 pmol/μl of an antisense oligonucleotide matching the 3′ end of the *jShak2* coding sequence 5′-(ACACTCTAGATAAGTGGTCACGTGATTTAACTCG)-3′. A second round used 5 pmol/μl of the T7 oligonucleotide and 25 pmol/μl of a nested antisense oligonucleotide near the pore region of *jShak2* 5′-(TCCGGTCGACGTAGAGGGGAATAAATCGCCATA)-3′. The product was cut with Xho I and Nhe I and subcloned into the Xho I and Xba I sites in Bluescript II KS^+ (Stratagene, La Jolla). Three separate clones were sequenced in both directions to minimize the possibility of reporting PCR-introduced mutations.

Genomic structures were determined by high stringency PCR amplification of genomic DNA with several oligonucleotides flanking the coding regions of *jShak1* and *jShak2* and oligonucleotides internal to the coding sequence. In all cases, single bands were amplified. In instances where the product resulting from amplification of genomic DNA corresponded in size to a band amplified from the cDNA clone with the identical oligonucleotides, genomic restriction mapping was used to verify the identity of genomic product. In cases for which the size of the genomic band exceeded that of the cDNA, the genomic band was subcloned into the Sma I site of Bluescript II SK^+ and sequenced to confirm the existence and position of the intron.

Alignments and phylogenetic trees. The alignments used to produce the pairwise identity data were generated in Microgenie (Beckman, Palo Alto) and adjusted by eye. Alignments which were used to produce maximum parsimony trees based on the *jShak1*, *jShak2* and 9 triploblastic Vg K^+ channels representing the *Shaker, Shal, Shab,* and *Shaw* gene subfamilies were generated using the SEQSEE suite of programs (Wishart et al., 1994). Only sections of the T1 region and membrane spanning core (S1–S6) that have conserved lengths between the *Shaker, Shal, Shab,* and *Shaw* subfamilies were used for tree building. Trees were constructed by maximum parsimony, as implemented in the PAUP computer program (Swofford, 1993). Tree lengths were calculated using a step matrix that weighted changes between amino acids according to the minimum number of nucleotide changes that were necessary to achieve the change in amino acids. A heuristic search for trees was performed, using random addition to generate initial trees, tree bisection and reconnection for branch swapping. The consensus maximum parsimony tree shown in Figure 2 was constructed from the shortest 13 trees found in this search.

Construction of Xenopus *oocyte expression vectors.* The *jShak1* expression vector was generated by PCR amplification of a previously constructed *jShak1*-Bluescript II KS^+ subclone with two primers: a sense primer 5′-(GGGAGCTCGAGCCACCATGATGTTTGTAGCCACT)-3′ that replaces the 5′ UT sequence with a consensus translation initiation sequence (Kozak, 1987) and an internal primer 3′ of a unique internal Sac I site 5′-(AATCATAATCATTCATCG)-3′. The PCR product was then digested with Sac I and cloned into the *jShak1*-Bluescript KS^+ subclone digested with Sac I. The PCR amplified region was sequenced in both directions to confirm correct orientation and lack of PCR-introduced mutations. A truncated *jShak1* construct (*jShak1T*) that eliminates the first 23 predicted amino acids and replaces phenlyalanine 24 with an initiator methionine preceded by a consensus translational initiation sequence was constructed using the sense primer 5′-(GGGAGCTCCACCATGGAAGACAATGCAGA)-3′.

The *jShak2* construct was produced in two steps. First, an incomplete *jShak2* cDNA isolated in the original bank screen described above was cut with Nhe I and Not I and subcloned into an Spe I/Not I cut pBScMXT oocyte expression vector (Wei et al., 1994). The 5′ end was amplified with a sense oligonucleotide 5′-(TTACGAATTCCACCATGTTACCAGTTCTAACGCAAACG)-3′ which replaces the 5′ UT sequences with a consensus translation initiation sequence and the previously described pore region antisense oligonucleotide. This product was cut with Eco RI and Nhe I and subcloned into the vector produced in the first step (Eco RI/Nhe I cut). The amplified region was sequenced in both directions to confirm that no PCR-introduced mutations existed.

Expression of cRNA in Xenopus *oocytes.* Capped cRNAs were prepared by run-off transcription with either T7 RNA polymerase (for *jShak1* and *jShak1T*), or with T3 RNA polymerase (*jShak2, Shaker H37, Shaker B,* and *Kv1.2*) using the mMessage mMachine kit (Ambion, Austin). Mature stage IV *Xenopus* oocytes were prepared for injection as described in Wei et al., 1990. Oocytes were injected with 50 nl of cRNA at concentrations of 5–100 ng/μl (adjusted based on the expression level of the particular construct), and incubated at 15°C for 1–3 d in ND96 (96 mM NaCl, 2 mM KCl, 1.8 mM $CaCl_2$, 1 mM $MgCl_2$, 5 mM HEPES-NaOH, pH 7.5) supplemented with 100 U/ml penicillin, 100 μg/ml streptomycin and 2.5 mM sodium pyruvate.

Electrophysiology. Recording methods used were as previously published in Covarrubias et al., 1991. Briefly, whole cell recordings were made 1–3 d after injection at 22°C by conventional two microelectrode voltage-clamp techniques. Electrodes ranged from 0.3–0.8 MΩ resistance and were filled with 3 M KCl. The standard recording solution consisted of ND96 with 1 mM 4,4′-diisothiocyanatostilbene-2,2′ disulfonic acid (DIDS) to block native oocyte chloride currents. Tetraethylammonium (TEA) and 4-aminopyridine (4-AP) were dissolved in this standard solution at the given concentrations. Currents were digitally acquired with CCURRENT using linear leak subtraction, filtered at 1 kHz with an 8-pole Bessel filter and analyzed with CQUANT (Baker and Salkoff, 1990).

Results

Cloning of jShak1 *and* jShak2

We designed a PCR-based method to screen for jellyfish Vg K^+ channel homologs that relied only on short stretches of conservation and compensated for differences in codon bias by using degenerate primers. We chose one degenerate primer to match the amino acid sequence of the K^+-selective pore region (Hartmann et al., 1991; Yellen et al., 1991; Yool and Schwarz, 1991) which is highly conserved in all the Vg K^+ channels (MTTVGYGD) as well as most other K^+ channels. The antisense primer matched a stretch of S6 (GVL(T/V)IAL), the most highly conserved membrane-spanning domain, which is invariant in *Shaker, Shal, Shab,* and *Shaw* (Wei et al., 1990). We used the same low stringency amplification protocols described in Jegla and Salkoff (1995) in which novel *Paramecium* K^+ channel clones were isolated starting with these primers. Using this screen, fragments of two jellyfish Vg K^+ channels, *jShak1* and *jShak2,* were isolated from *Polyorchis penicillatus* genomic DNA. These fragments were then used as a probe to isolate complete clones of *jShak1* and *jShak2* from a *Polyorchis penicillatus* cDNA library, as described in the Materials and Methods section.

Conservation with triploblastic Shaker *channels*

An alignment of the deduced amino acid sequences of *jShak1* and *jShak2* to triploblastic *Shaker* homologs from *Drosophila*

Table 1. Percent conservation of amino acids between the jellyfish Vg K^+ channels *jShak1* and *jShak1* and triploblastic Vg K^+ channels

	jShak1	*jShak2*	*Shaker B*	*Mus Kv1.2*	*Shal*	*Shab*	*Shaw*
jShak1		50 (55)	48 (51)	49 (52)	45 (41)	44 (34)	42 (37)
jShak2	50 (55)		52 (51)	51 (53)	44 (44)	46 (29)	46 (35)
Shaker B	48 (51)	52 (51)		69 (88)	42 (48)	43 (33)	44 (41)

Percentage amino acid identities are shown for pairwise alignments between *jShak1, jShak2,* the *Drosophila Shaker B* (Timpe et al., 1988a), *Shal, Shab,* and *Shaw* (Butler et al., 1989) Vg K^+ channels and the *Mus Shaker* homolog *Kv1.2* (McKinnon, 1989). Identities are measured from the first residue of S1 to the last residue of S6, and for the most highly conserved section of the T1 domain (shown in parentheses) corresponding to amino acids 47 through 126 in *jShak1.*

and *Mus* is shown in Figure 1. Extensive conservation between *jShak1, jShak2,* and triploblastic *Shaker* homologs extends from the T1 tetramerization domain (Li et al., 1992; Shen et al., 1993; Hopkins et al., 1994) in the N-terminal through the entire membrane-spanning core of the channels, which includes six transmembrane domains (S1–S6) and a K^+-selective pore motif. Note that conservation is particularly high in the pore and S6 regions to which our degenerate primers were made. Even the N-terminal "inactivation ball" region (Hoshi et al., 1990; Zagotta et al., 1990) shows limited sequence conservation. However, there is little conservation between *jShak1, jShak2,* and triploblastic *Shaker* homologs in the proximal N-terminal and distal C-terminal regions (which show little conservation even among triploblastic *Shaker* homologs).

In pairwise comparisons of the conserved core region (S1 through S6), *jShak1* and *jShak2* share approximately 50% amino acid identity to each other and to triploblastic *Shaker* homologs. This is less than the approximately 70% identity shared among triploblastic *Shaker* homologs (Salkoff et al., 1992; Jegla and Salkoff, 1994), but is higher than the approximately 40% level of identity conserved among *jShak1* and *jShak2* and the other voltage-gated K^+ channel subfamilies, *Shab, Shal,* and *Shaw.* This higher identity to *Shaker* versus *Shal, Shab,* or *Shaw* is even more pronounced in the T1 domain, and suggests that *jShak1* and *jShak2* are specifically *Shaker* homologs. A summary of these pairwise comparisons is provided in Table 1.

We constructed phylogenetic trees including *jShak1, jShak2* and 9 triploblastic Vg K^+ channel sequences from the *Shaker, Shal, Shab,* and *Shaw* subfamilies to confirm the inclusion of *jShak1* and *jShak2* within the *Shaker* subfamily, using the maximum parsimony computer program PAUP of Swofford (1993). A maximum parsimony consensus tree built from the 13 shortest (best) trees found by this program is shown in Figure 2. All 13 trees place *jShak1* and *jShak2* in the *Shaker* subfamily. In all trees, the two jellyfish *Shaker* channels diverge from the triploblastic *Shaker* homologs at an earlier time than the divergence of the triploblastic *Shakers* from each other, consistent with the early divergence of the diploblastic and triploblastic lineages. The consensus tree is consistent with the previous findings of Strong et al. (1993) in grouping the *Shaker* and *Shal* subfamilies. Less certain is whether the *Shaw* subfamily groups with the *Shab* subfamily (77%), as found by Strong et al. (1993), or the *Shal* subfamily (23%).

Multiple Shaker *genes and genomic organization*

As in vertebrates, *Shaker* is a multigene subfamily in *Polyorchis.* Gene duplication has produced a large set of *Shaker* genes with intronless coding regions in mammals (Chandy et al., 1990; Douglass et al., 1990; Swanson et al., 1990; Chandy and Gutman, in press), so we were interested to see if introns were present in *Polyorchis.* We examined the genomic structure of the *jShak1* and *jShak2* coding regions by PCR amplification of *Polyorchis* genomic DNA as described in the Materials and Methods. The coding region of *jShak1* appears to be intronless because no length differences are seen between the cDNA and genomic fragments encompassing the entire coding region. However, the *jShak2* coding region contains a single intron of approximately 1.2 kb in length in the region encoding the C-terminal cytoplasmic domain (Fig. 1, arrow).

Functional properties

Expression of cRNAs from *jShak1* and *jShak2* in *Xenopus* oocytes provides further evidence that *jShak1* and *jShak2* belong to the *Shaker* subfamily. Both *jShak1* and *jShak2* produced currents that resemble triploblastic invertebrate *Shaker* currents with respect to rapid activation and inactivation. Figure 3 shows a comparison of families of outward currents recorded from oocytes injected with *jShak1, jShak2,* and two *Drosophila* splice variants, *Shaker B* (Timpe et al., 1988a) and *Shaker H37* (Kamb et al., 1988). The biophysical and pharmacological properties of these currents are summarized in Table 2.

Although the *jShak1* and *jShak2* currents differ substantially in their rates of inactivation (Fig. 4*A*), both fall within the range of inactivation rates observed for different splice variants of *Drosophila Shaker* (Fig. 4*B*). Plots of the major time constant of inactivation (Tau) versus voltage are shown in Figure 4*C*. *JShak1* is most similar to the rapidly inactivating *Drosophila Shaker* splice variants (e.g., *Shaker B*), whereas *jShak2* has an inactivation rate similar to the more slowly inactivating *Shaker* currents such as *Shaker H37* and *Aplysia Shaker* (Pfaffinger et al., 1991). For these slower inactivating types, the inactivation time constant is greater than 20 msec at +60 mV. *JShak1* is also similar to *Drosophila Shaker B* in having a small sustained current component that does not inactivate over short voltage steps (Fig. 4*A*) (Timpe et al., 1988a,b; Isacoff et al., 1990). In contrast, *JShak2* inactivates completely during shorter steps, similar to *Shakers A* and *C* (Timpe et al., 1988a,b; Isacoff et al., 1990).

Because there is no significant conservation among the N-terminal regions of most triploblastic *Shaker* channels, we were surprised to observe substantial conservation between the N-terminal of *jShak1* and the *Drosophila Shaker B* channel (Fig. 5*A*). The fast component of inactivation in *Shaker B* occurs by an N-terminal "ball and chain" mechanism (Hoshi et al., 1990; Zagotta et al., 1990); when this region is removed, rapid inactivation of the current is lost. To test the functional significance

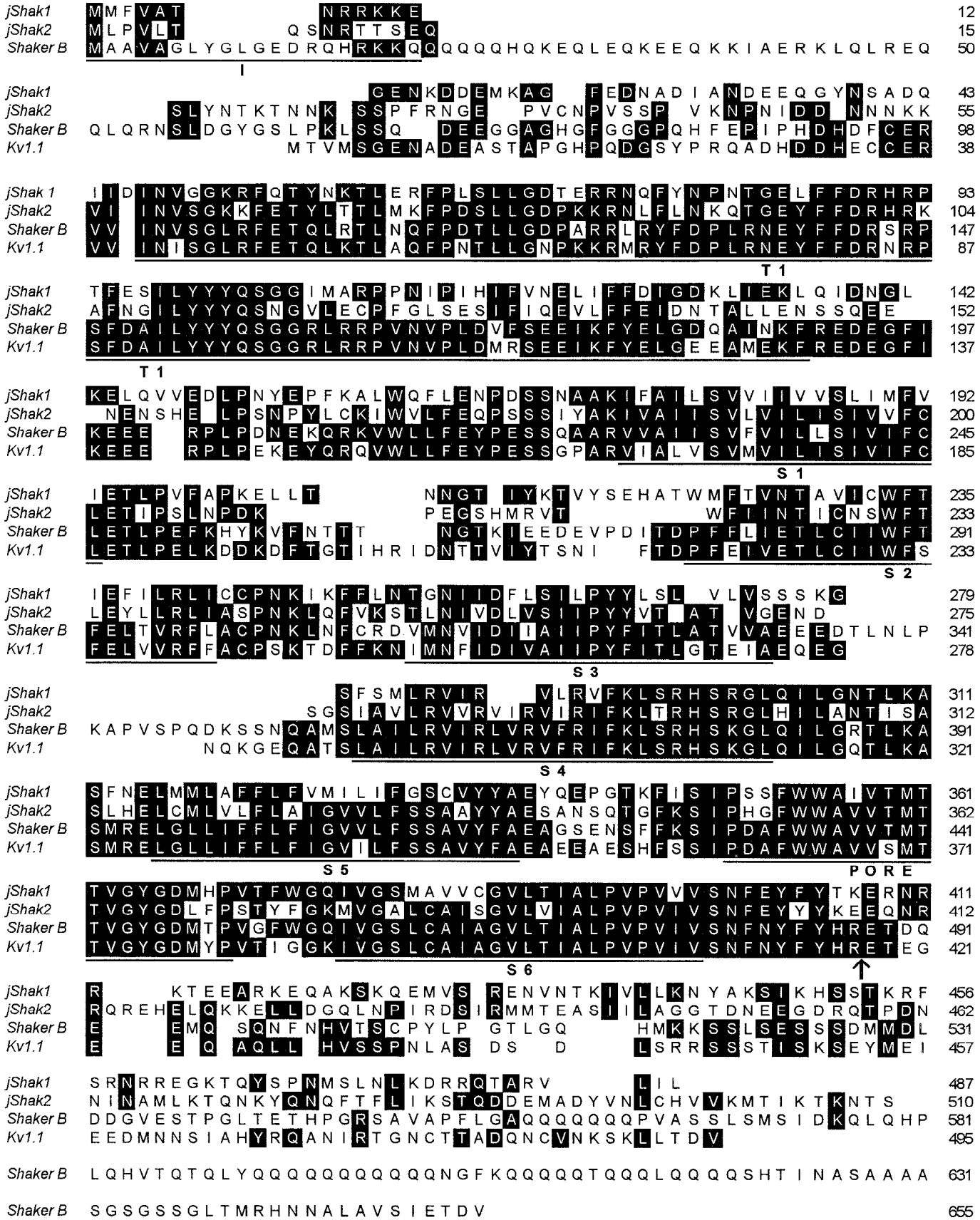

Figure 1. Alignment of the deduced amino acid sequences of the *jShak1, jShak2, Drosophila Shaker B* (Timpe et al., 1988a) and the mouse *Shaker* homolog *Kv1.1* (Tempel et al., 1988). Identical amino acids are shown in *reversed lettering* (white on black). Membrane-spanning domains are *underlined* and labeled S1 through S6. Also *underlined* are the putative pore-forming region (Pore), the N-terminal inactivation ball of *Shaker*

of the conservation between *jShak1* and *Shaker B,* we removed the first 23 amino acids of *jShak1* and expressed the truncated construct (*jShak1T*). As with *Shaker B,* the truncation completely removed rapid inactivation (Fig. 5*B,C*) from the *jShak1* current. This result demonstrates the conservation of the N-terminal inactivation ball mechanism. Partial inactivation of the *jShak1T* current occurs during prolonged (3 sec) depolarizations, suggesting the presence of a second, possibly C-type, inactivation process (data not shown).

JShak1 and *jShak2* differ substantially in their rates of recovery from inactivation, with *jShak1* showing more rapid recovery (Fig. 6*A*). Both have two distinct time components to their recovery from inactivation (Table 2, Fig. 6*B,C*). Two separable components to recovery could suggest recovery from two inactivated states. The fast component of recovery for *jShak1* (Tau = 24.4 msec at −100 mV) is very similar to the rapid recovery of the *Shaker B* splice variant (Tau = 42.6 msec at −100 mV), which has mainly N-type inactivation. The slow component is similar to the recovery rate of the *Shaker H37* splice variant and could conceivably reflect recovery from C-type inactivation (Fig. 6*D*). Both *Drosophila Shaker* currents recover with a single exponential time course. The extremely slow recovery of the *jShak2* current is similar to the *Drosophila Shaker A* and *C* splice variants (Timpe et al., 1988b) and *Aplysia Shaker* (Pfaffinger et al., 1991).

One difference between the jellyfish *Shaker* currents and their triploblastic counterparts is that *jShak1* and *jShak2* both operate in a more positive voltage range. *JShak1* and *jShak2* have conductance versus voltage (gV) relations and steady state inactivation (ssi) relations that show a depolarized shift with respect to those of typical triploblastic *Shaker* homologs (Fig. 7). The magnitude of this shift relative to oocyte-expressed *Shaker* currents in other species is approximately +25 mV for the ssi curves and almost +40 mV for the gV curves. *Drosophila Shaker* currents, however, can exhibit equally large shifts in their voltage operating range within some cell types (Hevers and Hardie, 1995).

An additional observation of interest is that the apparent voltage sensitivity differs substantially between the jellyfish and triploblastic *Shakers.* Both *jShak1* and *jShak2* show a lower voltage sensitivity when compared to triploblastic *Shaker* homologs by three measures: a reduced slope of the gV curve, a reduced limiting slope (which presumably provides a lower limit estimate on the number of equivalent gating charges (z) required to open the channel (Almers, 1978; Armstrong, 1981; Logothetis et al., 1992), and a reduced slope of the ssi curve (which may reflect the steepness of the voltage dependence of activation; Papazian et al., 1991); see Figure 7 and Table 2. Each of these measures suggests a reduction of voltage dependence of approximately 30%. These differences apparently do not reflect a difference in the number of gating charges in the S4 region. All higher metazoan *Shakers* as well as *jShak2* have seven positive charges in the S4 region. *JShak1,* on the other hand, has only six S4 charges (Fig. 1).

JShak1 and *jShak2* have pharmacological properties typical of *Shaker* currents. Both are similarly sensitive to block by 4-aminopyridine (having an IC_{50} of 0.5 mM or less), but differ 20-fold

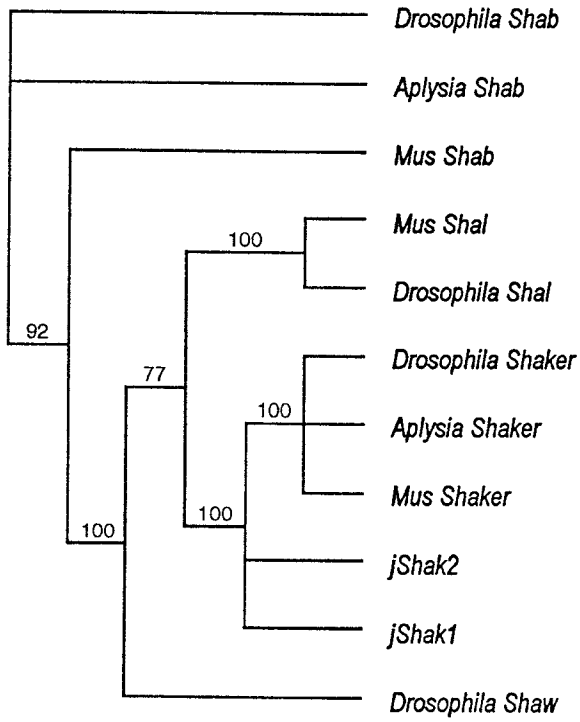

Figure 2. Consensus maximum parsimony tree derived from *jShak1, jShak2,* and nine triploblastic Vg K^+ channels representing the *Shaker, Shal, Shab,* and *Shaw* gene subfamilies. Numbers represent the percentage of occurrences of a particular branch point in the individual maximum parsimony trees used to construct this consensus tree. The references and accession numbers for the sequences used are as follows: *Drosophila Shaker* (Papazian et al., 1987; M17211) *Drosophila Shal, Drosophila Shab,* and *Drosophila Shaw* (Butler et al., 1989; M32660, M32659, M32661, respectively); *Mus Shaker* (Tempel et al., 1988; Y00305), *Mus Shal* (Pak et al., 1991; M64226), *Mus Shab* (Pak et al., 1991b; M64228), *Aplysia Shaker* (Pfaffinger et al., 1991; M95914), *Aplysia Shab* (Quattrocki et al., 1994; S68356).

in their sensitivity to block by externally applied TEA. While *jShak1* has an IC_{50} of 20 mM for external TEA, *jShak2* has an IC_{50} of approximately 1 mM. This difference is most likely explained by the presence of phenylalanine at position 370 in the pore region of *jShak2* as opposed to the histidine found in the equivalent position in *jShak1.* It has previously been reported that the presence of an aromatic amino acid at this position confers high external TEA sensitivity as seen for *jShak2,* whereas other amino acids result in lowering or abolishing sensitivity to external TEA (Heginbotham and MacKinnon, 1992).

Discussion

Sequence conservation

Phylogenetic sequence analysis clearly places the jellyfish K^+ channels *jShak1* and *jShak2* within the *Shaker* gene subfamily of Vg K^+ channels. Thus, the *Shaker* gene subfamily must have diverged from ancestral Vg K^+ channels prior to the evolutionary split between diploblasts and triploblasts. It is therefore likely that *Shaker* K^+ channels were already playing significant roles in the electrical activity of the earliest metazoan nervous sys-

←

B (I), and the N-terminal subunit assembly domain (T1). The *underlined* T1 domain includes the overlap of the critical subunit assembly regions determined in Li et al., 1992; Shen et al., 1993; and Hopkins et al., 1994). An arrow marks the position of an intron in the coding region of *jShak2.* The Genbank accession numbers of the *jShak1* and *jShak2* sequences are U32922 and U32923, respectively.

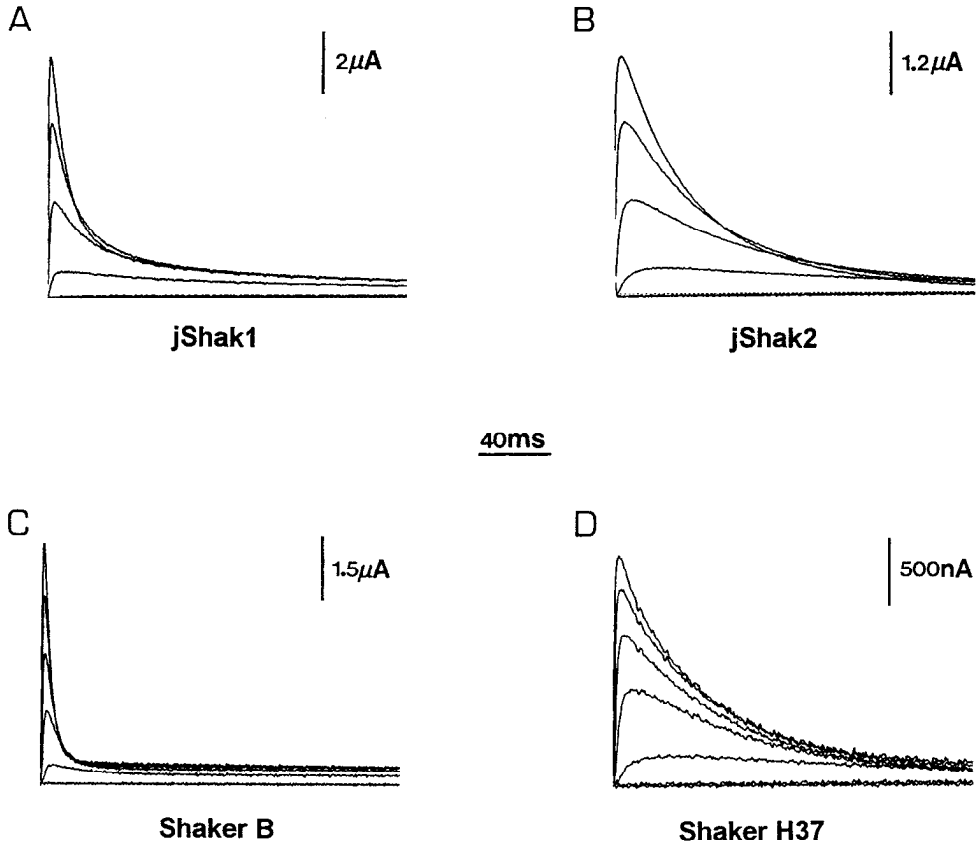

Figure 3. Families of outward currents recorded from *Xenopus* oocytes injected with cRNAs from *jShak1* (*A*), *jShak2* (*B*), *Drosophila Shaker B* (*C*), and *Drosophila Shaker H37* (*D*); 200 msec test pulses were applied from −40 mV to +60 mV in 20 mV increments for *jShak1* and *jShak2*, or from −60 mV to +60 mV in 20 mV increments for *Shaker B* and *Shaker H37*. Holding potentials were −90 mV and each pulse was preceded by a 6 sec prepulse to −130 mV to allow for complete recovery from inactivation between pulses. Current amplitude calibration bars are shown for each set of traces, and a time calibration bar is also provided. Currents were leak subtracted, and capacitative transient currents were clipped.

tems. This suggests that the establishment of a specialized set of Vg ion channels to control electrical signaling was one of the early molecular innovations in metazoan evolution. Additional support for this idea comes from recently obtained evidence that two jellyfish *Shal* homologs, a putative *Shaw* homolog, and a third *Shaker*-related gene may exist in *Polyorchis penicillatus* (Jegla and Salkoff, unpublished observations). Other classes of Vg ion channels also appear to have early origins in metazoans since a scyphozoan jellyfish Na^+ channel which is homologous to triploblastic Vg Na^+ channels has been described (Anderson et al., 1993).

In other experiments to explore the evolutionary origins of

Table 2. Summary of the biophysical and pharmacological properties of the jellyfish K^+ channels *jShak1* and *jShak2* compared to selected triploblastic *Shakers*

	jShak1	*jShak2*	*K v1.2*	*Shaker B*	*Shaker H37*
Activation					
V_{50} (mV)	20.2 ± 0.3 (n = 17)	22.2 ± 0.2 (n = 14)	−15.2 ± 0.5 (n = 6)		−19.6 ± 0.4 (n = 6)
Slope (mV/*e*)	12.3 ± 0.3 (n = 17)	11.4 ± 0.2 (n = 14)	8.4 ± 0.4 (n = 6)		8.3 ± 0.3 (n = 6)
Limiting slope	3.51 ± 0.04 (n = 5)	4.04 ± 0.11 (n = 11)	5.84 ± 0.35 (n = 6)		5.37 ± 0.19 (n = 4)
Inactivation					
V_{50} (mV)	−20.6 ± 0.2 (n = 9)	−18.9 ± 0.1 (n = 19)		−44.0 ± 0.2 (n = 7)	−43.5 ± 0.1 (n = 6)
Slope (mV/*e*)	6.2 ± 0.1 (n = 9)	5.2 ± 0.1 (n = 19)		3.9 ± 0.2 (n = 7)	2.8 ± 0.1 (n = 6)
Tau (msec)	8.9 ± 0.2 (n = 9)	35.1 ± 1.4 (n = 13)		3.5 ± 0.1 (n = 8)	41.5 ± 1.6 (n = 6)
Tau_{r-f} (msec)	24.4 ± 2.6 (n = 5)	245 ± 7.7 (n = 7)		42.6 ± 2.0 (n = 8)	
Tau_{r-s} (msec)	855 ± 56	2075 ± 60			1047 ± 81 (n = 2)
% Tau_{r-f}	43.4 ± 4.5	26.2 ± 1.6			
Pharmacology					
TEA IC_{50} (mM)	20.0 ± 2.5 (n = 4)	1.2 ± 0.1 (n = 8)		17.0 ± 3.4 (n = 3)	
4-AP IC_{50} (mM)	0.5 ± 0.2 (n = 4)	≈0.1 (n = 4)		1.5 ± 0.6 (n = 4)	

Biophysical and pharmacological properties of *jShak1* and *jShak2* are compared to those of two *Drosophila Shaker* splice variants (*B* and *H37*) and the *Mus Shaker* homolog *Kv1.2*. The V_{50} and slope (in mV/*e*-fold change in conductance) of activation and inactivation are derived from the Boltzmann fits of the gV and steady state inactivation data shown in Figure 7, *A* and *C*, respectively. The limiting slopes of activation were derived from the linear regression fits to the semilogarithmic plots of gV curves shown in Figure 7*B*. Tau is the time constant of inactivation and values were determined for the major component of inactivation at +60 mV. Tau_{r-f} and tau_{r-s} are the time constants of the fast and slow components of recovery from inactivation at −100 mV. The percentage of the total current that recovers with a time constant of tau_{r-f} is also given. IC_{50} values for external tetraethylammonium (TEA) and 4-aminopyridine (4-AP) represent the concentration at which the current is reduced to one-half the amplitude of the current in the absence of TEA or 4-AP. Values are ±SE; sample sizes are given in parentheses.

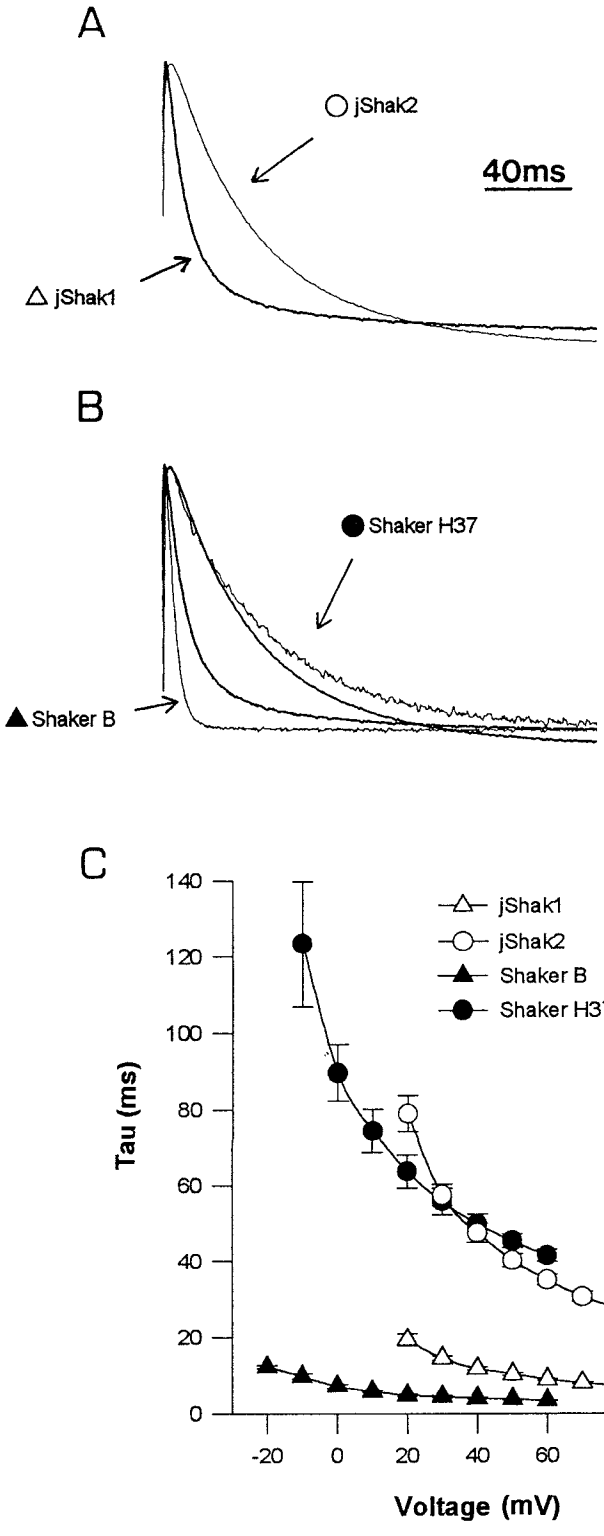

Figure 4. *JShak1* and *jShak2* have distinct inactivation rates. *A*, Differences in the inactivation rates of the *jShak1* and *jShak2* currents are illustrated by superimposing current traces from each; currents were elicited by 200 msec steps to +60 mV and normalized to the same peak amplitude. A time calibration bar is provided. *B*, Similar current traces from the *Drosophila Shaker* splice variants *B* and *H37* (*thin lines*) have been added to the *jShak1* and *jShak2* current traces (*thick lines*) shown in *A*. *C*, Plots of the major time constant of inactivation (tau) versus voltage are shown for *jShak1* (n = 9), *jShak2* (n = 13), *Shaker B* (n = 8), and *Shaker H37* (n = 6). Error bars show the SE of the data points.

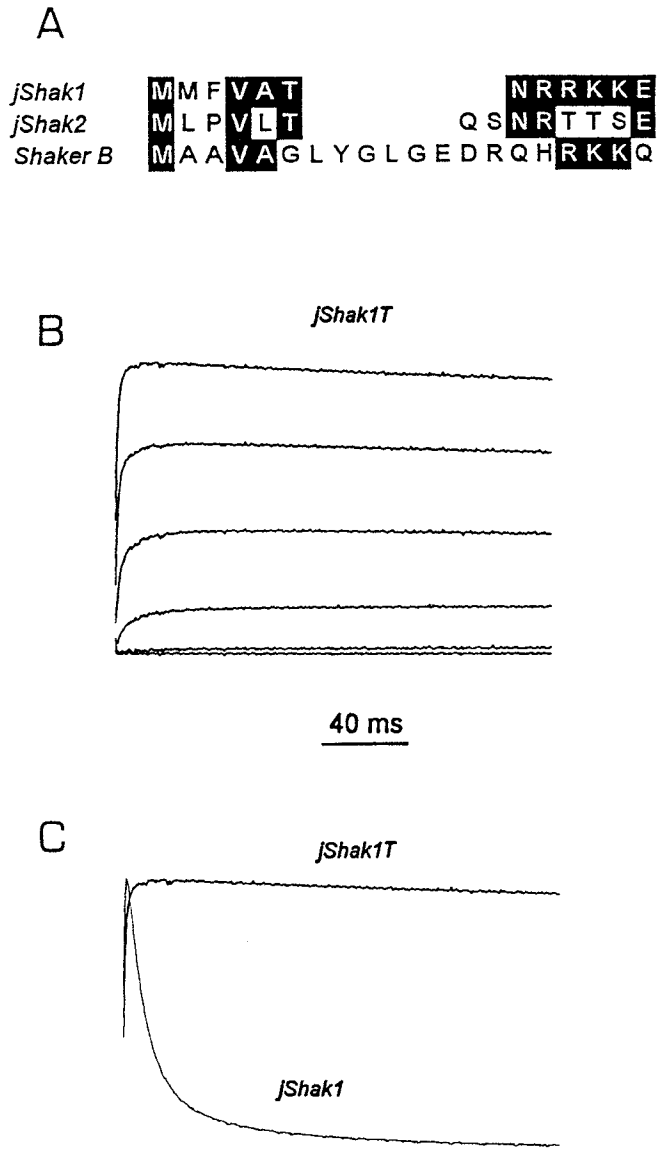

Figure 5. Rapid inactivation of *jShak1* occurs by a conserved N-terminal mechanism. *A*, An alignment of the first 12 amino acids of *jShak1* with the N-terminal of *Drosophila Shaker B* and *jShak2* is shown. *White type on black* indicates amino acid conservation. *B*, Outward currents recorded from an oocyte injected with cRNA from a truncated *jShak1* construct, *jShak1T*, in response to 200 msec depolarizations from −40 mV to +60 mV in 20 mV increments from a holding potential of −90 mV (peak current at +60 mV is 3.4 μA). Currents were leak subtracted and capacitative transient currents were clipped. *JShak1T* was constructed by removing the first 23 amino acids of *jShak1* (see Materials and Methods) *C*, 200 msec current traces elicited by depolarization to +60 mV and normalized to the same peak amplitude are shown for *jShak1* and *jShak1T*. The time calibration bar is for both *B* and *C*.

voltage-gated K^+ channels, an identical PCR screening method to that used here failed to reveal close homologs of the *Shaker*-like Vg K^+ channels in the electrically excitable ciliate protozoan *Paramecium tetraurelia*. Instead, that screen revealed a large family of novel K^+ channel genes in *Paramecium* that has only a very ancient relationship to *Shaker*-like channels (Jegla and Salkoff, 1995). Thus, it may be that the establishment of *Shaker*-like K^+ channels as a distinct subclass of Vg channels is tied to the emergence of metazoans or their direct ancestors,

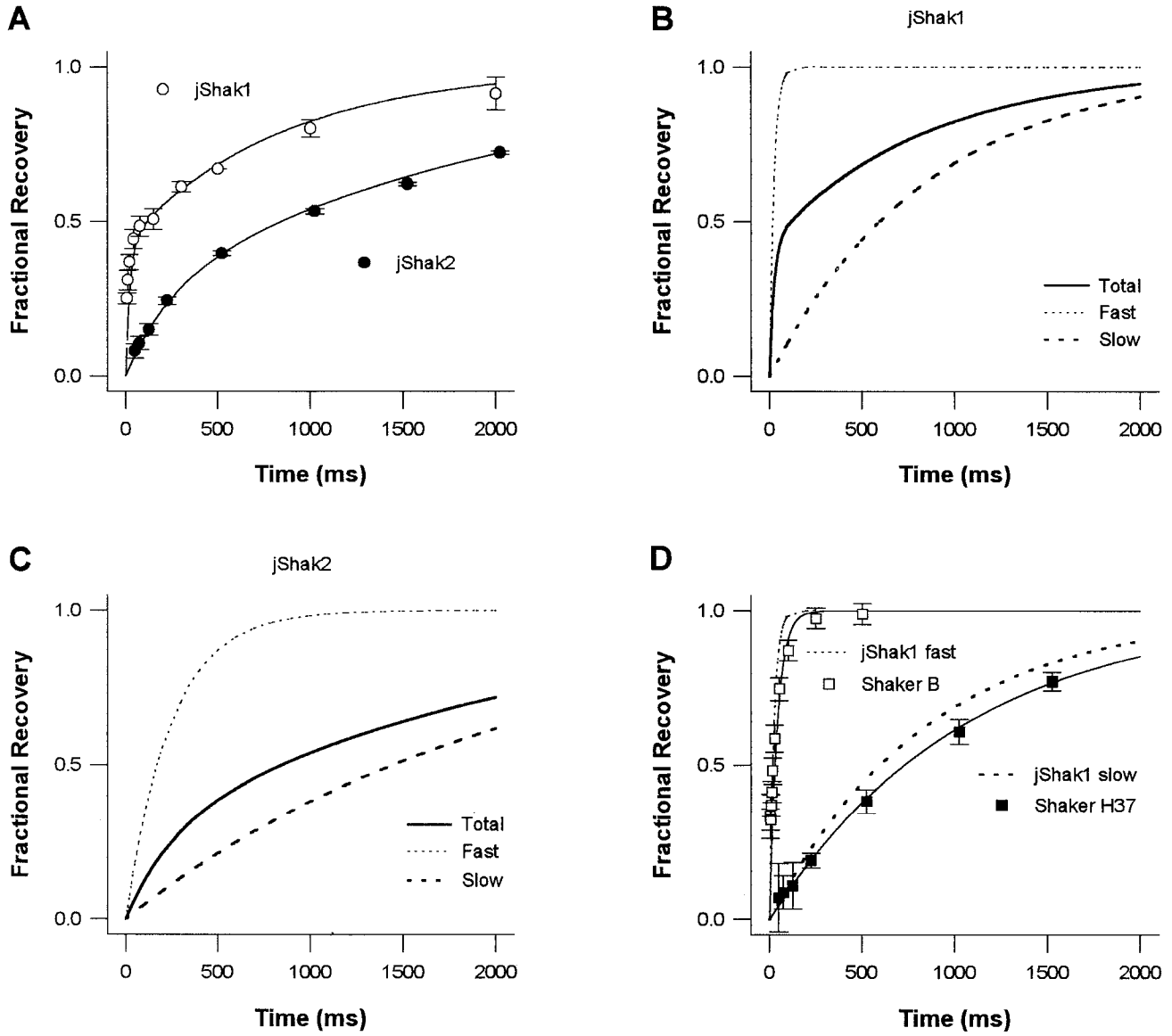

Figure 6. Recovery from inactivation. Curves fitting recovery from inactivation data for *jShak1* and *jShak2* at −100 mV are shown (*A*). Error bars show the SE of the data points. All recovery rates were determined in CQUANT using double pulse protocols in which two 200 msec pulses to +40 mV were separated by a pulse to −100 mV of increasing duration. Holding potentials were −100 mV and pulse series were separated by 6 sec intervals at −130 mV to ensure complete recovery from inactivation. Curves were generated using the equation $I_t = \{a\cdot(1 - \exp(-t/\text{tau1}))\} + \{b\cdot(1 - \exp(-t/\text{tau2}))\}$ where I_t is the current amplitude measured in the second +40 mV pulse divided by the current amplitude measure in the first pulse where t is the length of the recovery step at −100 mV, and a and b are the fractions of the total current recovering exponentially with time constants of tau1 and tau2, respectively. The values of *a, b,* tau1, and tau2 are shown in Table 2. Plots of the total recovery rate and the separated fast and slow components of recovery are individually shown for *jShak1* (*B*) and *jShak2* (*C*). Curves for each individual exponential component of recovery were normalized to the same amplitude as the total recovery, and were generated using the equation $I_t = 1 - \exp(-t/\text{tau})$, where tau is the time constant reflecting the single rate of recovery. The fast and slow components of the recovery rate of *jShak1* are shown with plots of the recovery rates of *Drosophila Shaker B* and *Shaker H37* (*D*). The *Drosophila Shaker* curves were generated using the equation for a single exponential component of recovery.

and possibly to the earliest use of electrical signals for intercellular communication.

Despite our strong evidence that *jShak1* and *jShak2* belong in the *Shaker* gene subfamily, they share substantially less amino acid identity to each other and to previously cloned triploblastic *Shaker* homologs (around 50%) than the triploblastic *Shakers* share with each other (around 70%) in the core regions of the channels. This divergence may reflect a very ancient split but has not led to large functional differences: the *jShak1* and *jShak2* currents are surprisingly similar to their *Drosophila* and *Aplysia* counterparts, especially with regard to their rapid activation and inactivation (Fig. 3). Thus much of this additional divergence appears neutral with respect to the functional properties that we have measured.

The lower level of conservation between *jShak1* and *jShak2* relative to that shared among triploblastic *Shaker* channels suggests that these two genes may have been diverging for a much longer time than their triploblastic homologs. If these two lineages split very early in diploblast evolution, homologs of each might be expected to be found in other hydrozoans, if not in all

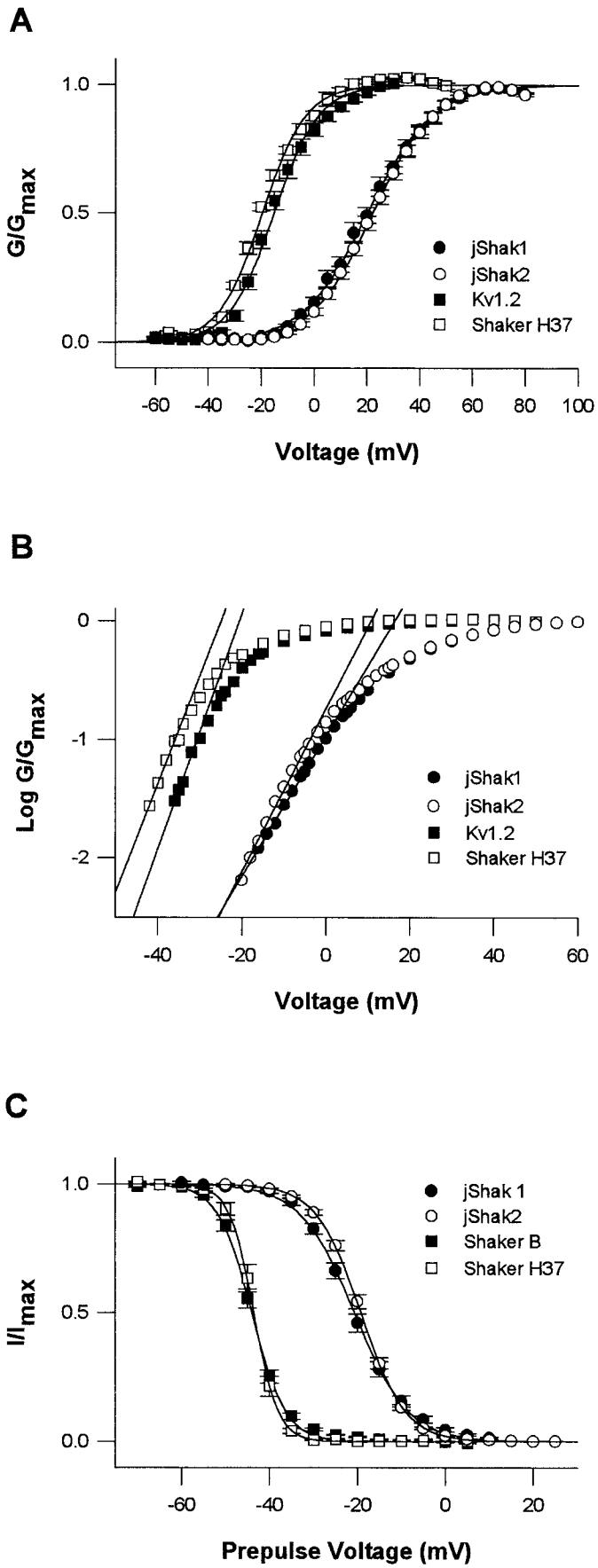

Figure 7. Voltage dependence of activation and inactivation. *A*, Conductance versus voltage curves (gV) are shown for *jShak1* (n = 16), *jShak2* (n = 14), *Drosophila Shaker H37* (n = 6), and mouse *Kv1.2* (n = 6). Error bars show the SE of the data points and solid curves represent Boltzmann fits of the data ($G/G_{max} = 1/(1 + \exp(-(V - V_{50})/a)$), where G is the conductance at voltage V, G_{max} is the maximal conductance, V_{50} is the voltage at which $G = 0.5 \cdot G_{max}$, and a is the slope factor. Conductances were determined by correcting peak current for driving force (reversal potential was assumed to be −90 mV in the ND96 recording solution). Test pulse durations were 100 msec for *jShak1*, 200 msec for *jShak2* and *Shaker H37*, and 400 msec for *Kv1.2*. Holding potentials and prepulses were the same as described in Figure 3. *B*, Semilogarithmic plots of gV curves obtained in the same manner as in *A*, but with additional data points for voltages at low g values (*jShak1*, n = 5; *jShak2*, n = 11; *Shaker H37*, n = 4; *Kv1.2*, n = 6). Lines represent linear regression fits to the data points below 10% g_{max}, and represent the limiting slope of voltage dependence. The slopes of these lines were directly used to obtain lower limit estimates of the total gating valence z (Table 2) from the equation $z = RT/F \cdot \ln((G/G\text{max})/V$ where R is the gas constant, T is the absolute temperature, F is Faraday's constant, and $\ln((G/G\text{max})/V)$ is the slope of the linear regression fit. *C*, Steady state inactivation curves are shown for *jShak1* (n = 9), *jShak2* (n = 19), and the *Drosophila Shaker B* (n = 7) and *Shaker H37* (n = 6) splice variants. Currents were obtained by measuring the peak current during test pulses to +40 mV preceded by 5 sec prepulses to the voltage shown on the x-axis. Holding potentials were −90 mV and 6 sec steps to −130 mV were used between test pulses to provide complete recovery from inactivation. Error bars show the SE of the data points, and the curves represent best fits of the data to the Boltzmann function $I/I_{max} = 1/(1 + \exp((V - V_{50})/a)$, where I is the peak current measured during the test pulse after a prepulse to voltage V, I_{max} is the maximal current measured, V_{50} is the prepulse voltage at which $I = 0.5 \cdot I_{max}$, and a is the slope factor.

cnidarians, much like homologs of specific *Shaker* genes (*Kv1.1*, *Kv1.2*, etc.) are found throughout the vertebrate classes (Chandy and Gutman, in press).

Functional properties

The depolarizing shift in the gV and ssi curves of the *jShak1* and *jShak2* currents when compared to typical triploblastic *Shaker* currents is consistent with observations that several A-type K^+ currents recorded from cnidarian cells, including those of *Polyorchis*, show a positive shift in voltage dependence (Anderson and McKay, 1987; Dunlap et al., 1987; Holman and Anderson, 1991; Przysiezniak and Spencer, 1994). A similar positive shift has been described for a jellyfish Na^+ current (Anderson, 1987) and a calcium current from *Polyorchis* (Przysiezniak and Spencer, 1992). Whether a reduced voltage sensitivity (with respect to triploblastic *Shaker* currents) is also a general property of these jellyfish A-type currents, as it is for *jShak1* and *jShak2*, is not clear. However, an A-type current in *Polyorchis* motor neurons does appear to have a reduced voltage sensitivity (Przysiezniak and Spencer, 1994).

Shaker channel homologs produce a more variable set of currents than other types of Vg K^+ channel such as *Shal* or *Shab* (Salkoff et al., 1992), particularly with respect to rates of inactivation and recovery from inactivation. The differences seen between the *jShak1* and *jShak2* currents in both their rates of inactivation and recovery from inactivation parallel those seen in *Drosophila Shaker* currents. Different splice variants of *Drosophila Shaker* vary 10-fold in inactivation rates from *Shaker B* to *Shaker H37*. Recovery rate time constants of *Drosophila Shaker* currents fall into two groups: rapid, like *Shaker B* (40 msec at −100 mV) and slow, like *Shaker H37* or *Shakers A* and *C*, which take several seconds to recover at −140 mV (Timpe et al., 1988b). The *jShak1* current is most similar to *Shaker B* as it has rapid N-type inactivation and a rapid component to

recovery. The *jShak2* current, on the other hand, has a slower inactivation rate (like *Drosophila Shaker H37* or *Aplysia Shaker*) and has slow recovery from inactivation (like *Drosophila Shakers H37, A* and *C*). *Shaker* currents in mammals are even more variable, ranging from rapid inactivation and slow recovery in Kv1.4 (Stuhmer et al., 1989; Ramaswami et al., 1990) to no inactivation in several mammalian *Shaker* homologs (Christie et al., 1989; Stuhmer et al., 1989; Grissmer et al., 1990; Swanson et al., 1990). Auxiliary subunits appear to further increase the diversity of inactivation properties in mammalian *Shakers* (Rettig et al., 1994). Thus, a diversity of *Shaker* current types appears to have been conserved between diploblasts and triploblasts.

It would appear that nervous systems have used a variety of functionally distinct *Shaker* currents virtually since their inception, and therefore all or most metazoans require some method of producing *Shaker* current diversity. In our diploblast representative *Polyorchis, Shaker* diversity is, at least in part, produced by multiple genes, *jShak1* and *jShak2*. As in mammals, alternative splicing is probably not very important in varying the functional properties of these genes because the coding region *jShak1* is intronless and the coding region *jShak2* contains only one intron in the C-terminal cytoplasmic domain. In mammals, as many as eight *Shaker* homologs exist, but most appear to contain intronless coding regions (Chandy et al., 1990; Douglass et al., 1990; Swanson et al., 1990; Chandy and Gutman, in press), so that alternative splicing probably does not contribute appreciably to *Shaker* current diversity. In *Drosophila,* only one *Shaker* gene appears to exist (Salkoff et al., 1992), but extensive alternative splicing leads to a wide range of functional properties (Jan and Jan, 1990).

The selective pressure to provide a variety of *Shaker* currents is thus wide-spread among metazoan phyla. The reason for this *Shaker* current diversity is unknown, but may reflect the adaptability of the rapidly activating *Shaker* current to a variety of roles. For instance, *Shaker* currents are even found in nonexcitable cells such as T-lymphocytes (Grissmer et al., 1990). Future examinations of more primitive metazoans such as sponges (which have non-neuronal conducting systems; Mackie et al., 1983) and of protozoans presumed to have close evolutionary ties to metazoans will help to more closely determine the relationship between *Shaker*-like voltage-gated K^+ channels and the evolution of the nervous system.

References

Almers W (1978) Gating currents and charge movements in excitable membranes. Rev Physiol Biochem Pharmacol 82:96–190.

Anderson PAV (1987) Properties and pharmacology of a TTX-insensitive Na^+ current in neurones of the jellyfish *Cyanea capillata.* J Exp Biol 133:231–302.

Anderson PAV, McKay MC (1987) The electrophysiology of cnidocytes. J Exp Biol 133:215–230.

Anderson PAV, Holman MA, Greenberg RM (1993) Deduced amino acid sequence of a putative sodium channel from the scyphozoan jellyfish *Cyanea capillata.* Proc Natl Acad Sci USA 90:7419–7423.

Armstrong CM (1981) Sodium channels and gating currents. Physiol Rev 61:644–683.

Baker K, Salkoff L (1990) The *Drosophila Shaker* gene codes for a distinctive K^+ current in a subset of neurons. Neuron 2:129–140.

Butler A, Wei A, Baker K, Salkoff L (1989) A family of putative potassium channel genes in *Drosophila.* Science 243:943–947.

Chandy KG, Williams CB, Spencer RH, Aguilar BA, Ghanshani S, Tempel BL, Gutman GA (1990) A family of three mouse potassium channel genes with intronless coding regions. Science 247:973–975.

Chandy KG, Gutman GA. Voltage-gated K^+ channel genes. In: CRC handbook of receptors and channels (North PA, ed), in press.

Christen R, Ratto A, Baroin A, Perasso R, Grell KG, Adoutte A (1991) An analysis of the origins of metazoans, using comparisons of partial sequences of the 28s RNA reveals an early emergence of triploblasts. EMBO J 10:4999–5003.

Christie MJ, Adelman JP, Douglass J, North RA (1989) Expression of a cloned rat brain potassium channel in *Xenopus* oocytes. Science 244:221–224.

Covarrubias M, Wei A, Salkoff L (1991) *Shaker, Shal, Shab* and *Shaw* express independent K^+ current systems. Neuron 7:763–773.

Douglass J, Osborne PB, Cai YC, Wilkinson M, Christie MJ, Adelman JP (1990) Characterization of *RGK5,* a genomic clone encoding a lymphocyte channel. J Immunol 144:4841–4850.

Dunlap K, Takeda P, Brehm P (1987) Activation of a calcium-dependent photoprotein by chemical signaling through gap junctions. Nature 325:60–62.

Gallin WJ (1991) Sequence of an acidic ribosomal protein from the jellyfish *Polyorchis penicillatus.* Biochem Cell Biol 69:211–215.

Grissmer S, Dethlefs B, Wasmuth JJ, Goldin AL, Gutman GA, Cahalan MD, Chandy KG (1990) Expression and chromosomal localization of a lymphocyte K^+ channel gene. Proc Natl Acad Sci USA 87:9411–9415.

Hartmann HA, Kirsch GE, Drewe JA, Taglialatela M, Joho RH, Brown AM (1991) Exchange of conduction pathways between two related K^+ channels. Science 251:942–944.

Heginbotham L, MacKinnon R (1992) The aromatic binding site for tetraethylammonium ion on potassium channels. Neuron 8:483–491.

Hevers W, Hardie RC (1995) Serotonin modulates the voltage dependence of delayed rectifier and *Shaker* potassium channels in *Drosophila* photoreceptors. Neuron 14:845–856.

Holman M, Anderson PAV (1991) Voltage-activated ionic currents in myoepithelial cells from the sea anemone *Calliactis tricolor.* J Exp Biol 161:333–346.

Hopkins WF, Demas V, Tempel BL (1994) Both N- and C-terminal regions contribute to the assembly and functional expression of homo- and heteromultimeric voltage-gated K^+ channels. J Neurosci 14:1385–1393.

Hoshi T, Zagotta WN, Aldrich RW (1990) Biophysical and molecular mechanisms of *Shaker* potassium channel inactivation. Science 250: 533–538.

Isacoff E, Papazian D, Timpe L, Jan YN, Jan LY (1990) Molecular studies of voltage-gated potassium channels. Cold Spring Harbor Symp Quant Biol 55:9–17.

Jan LY, Jan YN (1990) How might the diversity of potassium channels be generated? Trends Neurosci 13:415–419.

Jegla T, Salkoff L (1994) Molecular evolution of K^+ channels in primitive eukaryotes. In: Molecular evolution of physiological processes (Fambrough DM, ed), pp 213–222. New York: Rockefeller UP.

Jegla T, Salkoff L (1995) A multigene family of novel K^+ channels from *Paramecium tetraurelia.* Recept Channels 3:51–60.

Johansen K, Wei A, Salkoff L, Johansen J (1990) A leech gene sequence homologous to *Drosophila* and mammalian *Shaker* K^+ channels. J Cell Biol 111:60a.

Kamb A, Tseng-Crank J, Tanouye MA (1988) Multiple products of the *Drosophila Shaker* gene may contribute to potassium channel diversity. Neuron 1:421–430.

Kim E, Day TA, Bennett JL, Pax RA (1995) Cloning, characterization and functional expression of a *Shaker*-related voltage-gated potassium channel gene from *Schistosoma Mansoni* (Trematoda: Digenea). Parasitology 110:171–180.

Kozak M (1987) At least six nucleotides preceding the AUG initiator codon enhance translation in mammalian cells. J Mol Biol 196:947–950.

Li M, Jan YN, Jan LY (1992) Specification of subunit assembly by the hydrophilic amino-terminal domain of the *Shaker* potassium channel. Science 257:1225–1230.

Logothetis DE, Shahla M, Satler C, Lindpaintner K, Nadal-Ginard B (1992) Incremental reductions of positive charge within the S4 region of a voltage-gated K^+ channel result in corresponding decreases in gating charge. Neuron 8:531–540.

Mackie GO, Lawn ID, Pavans de Ceccatty M (1983) Studies on hexactinellid sponges II. Excitability, conduction and coordination of responses in *Rhabdocalyptus dawsoni.* Philos Trans R Soc Lond [Biol] 301:401–418.

McKinnon D (1989) Isolation of a cDNA clone coding for a putative second potassium channel indicates the existence of a gene family. J Biol Chem 264:8230–8236.

Meech RW, Mackie GO (1993) Potassium channel family in the giant motor axons of *Aglantha digitale*. J Neurophysiol 69:894–901.

Morris SC (1993) The fossil record and the early evolution of the Metazoa. Nature 361:219–225.

Pak MD, Baker K, Covarrubias M, Butler A, Ratcliffe A, Salkoff L (1991a) *mShal*, a subfamily of A-type K^+ channel cloned from mammalian brain. Proc Natl Acad Sci USA 88:4386–4390.

Pak MD, Covarrubias M, Ratcliffe A, Salkoff L (1991b) A mouse brain homologue of the *Drosophila Shab* K^+ channel with conserved delayed rectifier properties. J Neurosci 11:869–880.

Papazian DM, Schwarz TL, Tempel BL, Jan YN, Jan LY (1987) Cloning of genomic and complementary DNA from *Shaker*, a putative potassium channel gene from *Drosophila*. Science 237:749–753.

Papazian DM, Timpe LC, Jan YN, Jan LY (1991) Alteration of voltage-dependence of *Shaker* potassium channel by mutations in the S4 sequence. Nature 349:305–310.

Pfaffinger PJ, Furukawa Y, Zhao B, Dugan D, Kandel ER (1991) Cloning and expression of an *Aplysia* K^+ channel and comparison with native *Aplysia* K^+ currents. J Neurosci 11:918–927.

Pongs O (1993) *Shaker*-related K^+ channels. Sem Neurosci 5:93–100.

Przysiesniak J, Spencer AN (1992) Voltage-activated calcium currents in identified neurons from a hydrozoan jellyfish, *Polyorchis penicillatus*. J Neurosci 12:2065–2078.

Przysiesniak J, Spencer AN (1994) Voltage-activated potassium currents in isolated motor neurons from the jellyfish *Polyorchis penicillatus*. J Neurophysiol 72:1010–1019.

Quattrocki EH, Marshal J, Kaczmarek LK (1994) A *Shab* potassium channel contributes to action potential broadening in peptidergic neurons. Neuron 12(1):73–86.

Ramaswami M, Gautam M, Kamb A, Rudy B, Tanouye M, Mathew MK (1990) Human potassium channel genes: molecular cloning and functional expression. Mol Cell Neurosci 1:214–223.

Rettig J, Heinemann SH, Wunder F, Lorra C, Parcej DN, Dolly JO, Pongs O (1994) Inactivation properties of voltage-gated K^+ channels altered by presence of β-subunit. Nature 369:289–294.

Rudy B (1988) Diversity and ubiquity of K^+ channels. Neuroscience 25:729–749.

Rudy B, Kentros C, Vega-Saenz de Miera E (1991) Families of potassium channel genes in mammals: toward an understanding of the molecular basis of potassium channel diversity. Mol Cell Neurosci 2:89–102.

Salkoff L, Baker K, Butler A, Covarrubias M, Pak MD, Wei A (1992) An essential set of K^+ channels conserved in flies, mice and humans. Trends Neurosci 15:161–166.

Shen NV, Chen X, Boyer MM, Pfaffinger PJ (1993) Deletion analysis of K^+ channel assembly. Neuron 11:67–76.

Strong M, Chandy KG, Gutman GA (1993) Molecular evolution of voltage-sensitive ion channel genes: on the origins of electrical excitability. Mol Biol Evol 10:221–242.

Stuhmer W, Ruppersberg JP, Schroter KH, Sakmann B, Stocker M, Glese KP, Perschke A, Baumann A, Pongs O (1989) Molecular basis of functional diversity of voltage-gated potassium channels in mammalian brain. EMBO J 8:3235–3244.

Swanson RA, Marshall J, Smith JS, Williams JB, Boyle MB, Folander K, Luneau CJ, Antanavage J, Oliva C, Buhrow SA, Bennet C, Stein RB, Kaczmarek LK (1990) Cloning and expression of cDNA and genomic clones encoding three delayed rectifier potassium channels in brain. Neuron 4:929–939.

Swofford DL (1993) Phylogenetic analysis using parsimony. Champaign, IL: Illinois Natural History Survey.

Tempel BL, Jan YN, Jan LY (1988) Cloning of a probable potassium channel gene from mouse brain. Nature 332:837–839.

Timpe LC, Schwarz TL, Tempel BL, Papazian DM, Jan YN, Jan LY (1988a) Expression of functional potassium channels from *Shaker* cDNA in *Xenopus* oocytes. Nature 331:143–145.

Timpe LC, Jan YN, Jan LY (1988b) Four cDNA clones from the *Shaker* locus of *Drosophila* induce kinetically distinct A-type potassium currents in *Xenopus* oocytes. Neuron 1:659–667.

Wainright PO, Hinkle G, Sogin ML, Stickel SK (1993) Monophyletic origins of the Metazoa: an evolutionary link with fungi. Science 260: 340–341.

Wei A, Covarrubias M, Butler A, Baker K, Pak M, Salkoff L (1990) Diverse K^+ currents expressed by a *Drosophila* extended gene family which is conserved in mouse. Science 248:599–603.

Wei A, Jegla T, Salkoff L (1991) A *C. elegans* potassium channel gene with homology to *Drosophila Shaw*. Soc Neurosci Abstr 17:1281 (s10.10).

Wei A, Solaro C, Lingle C, Salkoff L (1994) Calcium sensitivity of BK-type K_{ca} channels determined by a separable domain. Neuron 13: 671–681.

Wishart DS, Boyko RF, Willard L, Richards FM, Sykes BD (1994) SEQSEE: a comprehensive program suite for protein sequence analysis. Comp Appl Biosci 10:121–132.

Yellen G, Jurman ME, Abramson T, Mackinnon R (1991) Mutations affecting internal TEA blockade identify the probable pore-forming region of a K^+ channel. Science 251:939–942.

Yool AJ, Schwarz TL (1991) Alteration of ionic selectivity of a K^+ channel by mutation of the H5 region. Nature 349:700–704.

Zagotta WN, Hoshi T, Aldrich RW (1990) Restoration of inactivation in mutants of *Shaker* potassium channels by a peptide derived from *ShB*. Science 250:568–571.

Zhao B, Rassendren F, Kaang BK, Furakawa Y, Kubo T, Kandel ER (1994) A new class of noninactivating K^+ channels from *Aplysia* capable of contributing to the resting potential and firing pattern of neurons. Neuron 13:1205–1213.